J Photochem Photobiol B. Author manuscript; available in PMC 2016 October 12.

Published in final edited form as:
J Photochem Photobiol B. 2016 September ; 162: 412–420. doi:10.1016/j.jphotobiol.2016.07.001.

Hyperspectral imaging of snow algae and green algae from aeroterrestrial habitats

Andreas Holzinger[1,*], **Michael C. Allen**[2], and **Dimitri D. Deheyn**[2,*]

[1]Institute of Botany, Functional Plant Biology, University of Innsbruck, Sternwartestrasse 15, 6020 Innsbruck, Austria

[2]Marine Biology Research Division, Scripps Institution of Oceanography, University of California San Diego, 9500 Gilman Dr., La Jolla, CA 92093-0202 USA

Abstract

Snow algae and green algae living in aeroterrestrial habitats are ideal obbjects to study adaptation to high light irradiation. Here, we used a detailed description of the spectral properties as a proxy for photo-acclimation/protection in snow algae (*Chlamydomonas nivalis*, *Chlainomonas* sp. and *Chloromonas* sp.) and charopyhte green algae (*Zygnema* sp., *Zygogonium ericetorum* and *Klebsormidium crenulatum*). The hyperspectral microscopic mapping and imaging technique allowed us to acquire total absorbance spectra of these microalgae in the waveband of 400-900 nm. Particularly in *Chlamydomonas nivalis* and *Chlainomonas* sp., a high absorbance in the wave band of 400-550 nm was observed, due to naturally occurring secondary carotenoids; in *Chloromonas* sp. and in the charopyhte algae this was missing, the latter being close relatives to land plants. To investigate if cellular water loss has an influence on the spectral properties, the cells were plasmolysed in sorbitol or desiccated at ambient air. While in snow algae, these treatments did not change the spectral properties, in the charopyhte algae the condensation of the cytoplasm and plastids increased the absorbance in the lower waveband of 400 – 500 nm. These changes might be ecologically relevant and photoprotective, as aeroterrestrial algae are naturally exposed to occasional water limitation, leading to desiccation, which are conditions usually occurring together with higher irradiation.

Keywords

carotenoids; green algae; stress tolerance; hyperspectral imaging; pigments

1 Introduction

Snow algae and aeroterrestrial algae are naturally exposed to high photosynthetically active radiation (PAR) as well as ultra violet (UV) radiation, e.g. [1–3]. Such radiation is on the one hand necessary to drive photosynthesis, but on the other hand can produce deleterious effects when in excess. Hence, a variety of compounds (phenolic based but also others) associated with UV protection have been described in *Zygogonium ericetorum* [4–5] and

*Correspondence: Andreas.Holzinger@uibk.ac.at; ddeheyn@ucsd.edu.

Europe PMC Funders Author Manuscripts

Zygnema sp. [6]. In addition, mycosporine-like amino acids (MAAs, e.g. [7]) and certain cell-wall components may also be protective in green algae (for summary see [8]). As for snow algae, secondary pigments like the carotenoid astaxanthin, which is responsible for the red color of the spores ('red snow'), has substantial protecting capacities for the photosynthetic apparatus e.g. [1, 9–10]. Snow algae from the Chlamydomonadaceae usually have a life cycle that comprises mobile cells with flagella (swarmers) during early spring, when snow is melting, and allowing them to migrate to the surface of the snowpack [11]. Here, we investigate only the non-flagellated mature spore stages (formerly termed hypnoblasts) that have developed thick secondary walls and already lack the flagella; for origin and developmental stage, see Tab 1. The chemical composition of these pigments has been studied in detail [10–13], however their subcellular distribution was never clearly described. Pigment composition in red snow algae (*Chloromonas nivalis* and other Chlamydomonadaceae) and green snow algae (mostly containing *Microglena* sp.) collected from Svalbard (Norway) showed that primary carotenoids attributed only for 4% of the total pigments whereas the total secondary carotenoids comprised 92% of the pigments [12]. The pigment composition is developmental stage dependent in *Chloromonas nivalis* in which younger developmental stages contain contain less astaxanthins, giving them a green appearance; even mature spores of this genus turn only orange, but never fully ared [14]. In addition to pigments, snow algal spores of *Chlamydomonas nivalis* [1], *Chlainomonas* [10] or *Chloromonas nivalis* [14] are occasionally surrounded with organic and inorganic matter from the immediate surrounding environment, likely to prevent excessive irradiation in the snowfields.

Although the ecological roles of aeroterrestrial green algae are significant, only few studies have examined their adaptation mechanisms to extreme environmental stress [7, 15–23]. 'Hydroterrestrial' life forms of algae rely more directly on the availability of water than aeroterrestrial algae, but have the ability to occasionally fall dry which is when they are also exposed to a wide range of stresses [3, 24]. Thus, for the present study we do not distinguish between these life forms and summarize them as aeroterrestrial algae. It must also be stated that the aeroterrestrial algae used here were either cultured samples (*Klebsormidium crenulatum*, [15], *Zygnema* sp. [16] Tab. 1) or field-collected samples (*Zygogonium ericetorum* [17, 18]), and only vegetative cells were used for the investigations. A detailed knowledge of their spectral properties is crucial for understanding their survival strategies, since these algae are potentially exposed to full sunlight and high levels of deleterious radiation.

Hyperspectral imaging is a microscopy technique by which spectra can be spatially mapped. In other words, each pixel of a hyperspectral image contains the full spectrum of visible light (usually 400-900nm). The spectra of one single column of pixels are all acquired simultaneously, without the need to scanning. However, in order to build large (multi-columns of pixels) spectral maps, each column of pixels of interest is acquired and integrated into an image (which thus consists of many vertical lines of spectra acquisition). The spectral mode can be in reflectance, fluorescence, or absorbance, as the case here, thus leading to a spectral topography of the absorption patterns across the sample. The technique provides spatial mapping at sub-micron spatial resolution of spectra with < 2 nm wavelength resolution. Hyperspectral analysis is therefore critical for determining structures with

specific spectral properties, like absorbance or light scattering. The combination of optical options combined with the hyperspectral analysis can therefore associate spectral and ecological properties to specific structural parts. The technique of hyperspectral imaging has been widely used for space exploration and airborne mapping of land and coral reefs [25–31]; but only a few instruments have now been mounted on microscopes for fundamental research purposes.

In the present study, we focus for technical reasons on the absorption in the visible range above 400 nm, and record spectra up to 900 nm. The major pigments of green algae show different spectral properties and are therefore good candidates to be investigated for their distribution. While chlorophylls show two distinct absorption maxima, one between 400-500 nm and the second one between 600-700 nm, the absorption maxima of carotenoids can expand over 500 nm. We tested the feasibility of using the hyperspectral imaging technique in localization of different pigments, and we investigated the effect of structural changes caused by cellular water loss through plasmolysis or desiccation on the spectral properties. This novel approach provides new insights on the spectral properties of these organisms that have adapted to live in extreme habitats.

2 Material and Methods

2.1 Algal Material

2.1.1 Snow algae—Red snow samples containing snow algae (WP79) were collected in Kühtai, (11.05.2015 N47°13.422, E11°01.310 2300 m a.s.l.) or (S1) collected near Mt. Schönwieskopf (46°50.998 N, 11°00.903 E; 2350 m a.s.l., near Obergurgl, Ötztal, Austria. Life cells were transferred to the Scripps Institution of Oceanography (SIO, UC San Diego, La Jolla, California USA) within two days after sampling for further analyses. Cells were kept at low temperature (4°C) and low light intensity (~30 μmol photons m^{-2} s^{-1}).

2.1.2 Aeroterrestrial green algae—The aeroterrestrial green alga *Klebsormidium crenulatum* (SAG 2415, culture collection of algae in Göttingen, Germany, [15]) and freshly collected field samples of *Zygogonium ericetorum*, were from Mt. Schöwieskopf, near Obergurgl (for location see above, S1). *Zygnema* sp. (SAG 2419, [16]) was previously obtained from the sandy littoral zone of the river Saalach (N47°47.870, E12°56.4266; 440 m a.s.l.) near Salzburg, Austria. Life cells were transferred to the SIO within two days after sampling for further analyses. Cells were kept at 20 °C and low light intensity (~30 μmol photons m^{-2} s^{-1}).

2.2 Plasmolysis and desiccation experiments

Subsamples of the respective green algae have been plasmolysed in 800 mM or 1,600 mM sorbitol for 2 h at the SIO (according to [15, 17]). The plasmolysed samples were mounted in the plasmolysis solution for hyperspectral analysis. Desiccation was performed at ambient air, room temperature (20°C) and as routinely performed by the lead author [13, 16].

2.3 Light microscopy

Light microscopy of the algal strains under investigation was performed with a Nikon Eclipse 50i microscope, equipped with a Plan Fluor 40x 1.3 NA oil objective.

2.4 Hyperspectral imaging and calculation of the absorbance

The system used for this study (PARISS® hyperspectral imager, Light Form Inc.), is mounted on a Nikon Eclipse 80i microscope, with objectives from 4x to 100x, five sets of filter cubes for epifluorescence (one of which is optimized for chlorophyll), and the ability to look at samples in reflectance (specular and angular), transmission, dark field or phase contrast. Under each of these conditions, the hyperspectral imager acquires entire spectra simultaneously for every pixel of a column, which can be repeated as many times as needed to cover the area of interest. The PARISS® software identifies a set of spectra that are different from one another with the level of difference dictated by the Minimum Correlation Coefficient (MCC, see below). Each spectrum can then be assigned a coded color that can be mapped back to the area that was acquired. Thus the mapped images have a color-code that reflects the identity of corresponding spectra (and not the actual color of the sample).

3 Results

3.1 Light microscopy, plasmolysis and desiccation

The different snow algal samples had distinct content of genera. While in the sample from Obergurgl (S1) only *Chlamydomonas nivalis* was found, which contained inorganic debris and coating of the cells (Fig. 1 a), in the sample from Kühtai (WP79) different genera could be found (Fig. 1 b-c). The detected genera were *Chlamydomonas nivalis*, *Chlainomonas* sp. (Fig. 1 b), *Chloromonas rosae var. psychrophila* and *Chloromonas brevispina* (Fig. 1 c). When these samples were incubated in 1,600 mM sorbitol for 2 h virtually no visible change was detected (Fig. 1 d-e). Only when cells were desiccated, they showed a changed morphology with a dense appearance (Fig. 1 f).

In *Zygnema* sp. two stellate chloroplast are present in each cell with a central pyrenoid, with small vacuoles in the cell periphery (Fig. 2 a). When these cells were plasmolysed in 800 mM sorbitol for 2 h, a marked retraction of the protoplasts from the cell periphery was observed (Fig. 2 b). The retracted protoplasts were spherical in appearance, and the chloroplasts appeared condensed. When *Zygnema* sp. cells were desiccated under ambient air, irregular retraction of the protoplast from the surface was observed (Fig. 2 c). *Zygogonium ericetorum* contains two plate like chloroplast in each cell (Fig. 2 d), and upon air drying an irregular shrinkage of the cells was observed (Fig. 2 e). *Klebsormidium crenulatum* showed a similar behavior to plasmolysis [21] and desiccation [20] as previously illustrated, and is therefore not shown.

3.2 Hyperspectral imaging

3.2.1 Snow algae—Snow algae *Chlainomonas* sp. and *Chlamydomonas nivalis* showed a similar spectral pattern, with the highest absorption in the cell body (Fig. 3 a-c). High absorbance was found in the wave band between 400 -600 nm, and an additional peak at around 680 nm. Depending on the MCC (the higher the MCC value the greater the

discrimination between spectra with differences), MCC=0.985 (Fig. 3 b), MCC= 0.99 (Fig. 3 c), the appearance of the hyperspectral image varies only slightly, and identifying from 9 spectra (Fig. 3 b) to 11 spectra (Fig. 3 c). The additional spectra however did not affect significantly the spectral mapping, indicating that these new added spectra correlate well with the ones obtained with a lesser discriminatory power. Due to this, all further hyperspectral images were calculated with MCC=0.985. The field sample WP79 contains distinct cells, which were also clearly depicted by hyperspectral imaging (Fig. 3 d-e); not only the shape, but also the absorbance pattern were clearly distinct between *Chlamydomonas nivalis* and the two *Chloromonas* sp., which are lacking absorbance in the range between 500 – 600 nm (see blue and green spectra of Fig. 3 e). Field samples of *Chlamydomonas nivalis* S1 (Fig. 3 f), which were covered by inorganic debris, obviously hardly absorbing in the detected waveband (magenta to yellow area on hyperspectral mapping; Fig. 3 f, the cell center however showed a similar spectral profile of absorption as *Chlamydomonas nivalis* form WP79 (Fig. 3 e). The 'halo effect' with purple and red colors, shows little spectral absorbance, and is likely due to the surface coatings of these cells (compare Fig. 1 a). When snow algae were plasmolysed with 800 mM (Fig. 4 a-b) or 1,600 mM sorbitol (Fig. 4 c), no drastic change in the absorbance pattern was found. Desiccating snow algae at ambient air lead to accumulation of the cells into clumps with increased absorbance, particularly in the wavelength band below 600 nm (Fig. 4 d).

3.2.2 Aeroterrestrial green algae—In *Zygnema* sp. the spectral pattern observed in *Zygnema* sp. (Fig. 5 a-b) was clearly distinct from the investigated snow algae *Chlamydomonas* sp. and *Chlainomonas* sp. The highest values in the spectrum were found close to the lower detection limit of 400 nm, from there the absorbance dropped drastically, reaching a minimum at 500 nm. An additional peak was clearly found at around 680 nm. In untreated cells, the absorbance was fairly homogeneous throughout the cell towards the cell periphery (Fig. 5 b). When *Zygnema* sp. cells were plasmolysed in 800 mM sorbitol, a distinct retraction of the cytoplasm was observed. This resulted in a space between the cell wall and the cytoplasm, which had no absorbance and thus no associated spectra (hence the gray image with no mapped spectra; Fig. 5 c). The spectral properties in the waveband between 400 – 500 nm was changed slightly, the peak intensity at the 680 nm value was increased. An even more drastic effect was observed upon desiccation of *Zygnema* sp. filaments (Fig. 5 e). While the spectral properties did not change, the absorbance levels increased, likely due to the increased accumulation of pigments. In contrast, in *Zygogonium ericetorum*, no such increase was observed in the desiccated cells (Fig. 5 f). The parietal chloroplasts of *Klebsormidium crenulatum* gave a distinct spectral pattern (Fig. 6 a-b). The highest absorbance was found in the areas where this open ring of the chloroplast overlaps (Fig. 6 b). The total signal was weaker, possibly due to the smaller size of the cells. When *K. crenulatum* was plasmolysed with 800 mM sorbitol, a retraction of the cytoplasm was observed (Fig. 6 c), which was also seen in the hyperspectral image (Fig. 6 d).

4 Discussion

The hyperspectral imaging technique (PARISS®) used is attractive because it provides a spatial analysis of spectral information from live specimen of single-celled algae. This is

innovative in the sense that conventional techniques either (1) characterize the ultrastructure of fixed cells, use dyes to locate certain cellular compartments or (2) characterize spectra from cells after pigment extraction and spectral analysis from the extract. Hyperspectral imaging combines these two and seeks to provide spectral mapping from live cells, thus showing the possible interaction (based on respective localization) between organelles and pigments.

In the present study a hyperspectral characterization of snow algae (Chlorophyta) and aeroterrestrial green algae (Charophyta) was performed. The PARISS® technique allows one to fully map the spectral signal in a two dimensional chart, giving clear information where signals with a certain spectral property are located within the cells. A clearly different hyperspectral pattern was found in samples that contain abundant amounts of astaxanthin like mature spores (*Chlamydomonas nivalis*, *Chlainomonas* sp.) when compared to cells that contained visibly less secondary carotenoids, like the spores of *Chloromonas* sp. and chlorophyll-only containing algae (like *Klebsormidum*, *Zygnema*, *Zygogonium*). While secondary carotenoid containing snow algae had an absorption maximum in the waveband between 400 - 550 nm (which nicely goes along with the measured peak of the apolar keto-carotenoid isomer 13Z cis-astaxanthin in *Chlamydomonas nivalis* [9, 11], a drastic drop of the absorption was found in algae lacking this pigment. An additional peak has been observed in the range of 680 nm which is due to the chlorophyll absorbance (excitation wavelength of the chlorophyll fluorescence).

The PARISS® technique applied in this study has the advantage of simultaneously generating all the spectral information for one line of pixel, which by accumulating lines generates an hyperspectral image fairly quickly, especially in the absorbance mode (for our study, it took about 5 ms per line acquisition, thus less than 1 s to scan a large field of view). Thus, such conditions precluded from measuring photobleached conditions. Compare to other spectral analyses done from plant material (using two separate techniques such and micro-spectrophotometry in bright field -MSP, or Pulse Amplitude Modulated fluorometry - PAM), the hyperspectral imaging technique brings this unique spatial dimension to the spectra (both in bright field and fluorescence within the same instrument), which can be critical for understanding the ecology of some of these algae in relation to managing irradiance with other stressors. One of the challenges of this technique is to set the MCC properly in order to get a reasonable resolution of the different spectral properties; on the other hand, when the resolution is too detailed, the generated image gets difficult to read. In the present study, a MCC value of 0.985 turned out to be suitable and was used for image processing. In fact, the number of detected spectra increased from 9 (at MCC 0.985, Fig. 3 b) to 11 when setting the MCC value to 0.99 (Fig. 3 c). By further increasing this value, the number of discriminated spectra gets so high, that the two dimensional charts are getting extremely difficult to read.

4.1 Determination between different genera

Hyperspectral analysis is usually used to remotely identify species of plants [32–35], considering that the hyperspectral signature tends to be species specific. This was confirmed here between *Chlamydomonas* sp. vs. *Chloromonas* sp.. *Chlamydomonas nivalis* [1, 9–11]

and *Chlainomonas* sp. [11] have abundant secondary pigments like astaxanthins, giving them a red appearance. *Chloromonas nivalis* also contains astaxanthins, however young cells with a greener appearance contained less secondary pigments [14]. A similar situation might be the case in the here investigated *Chloromonas* sp. with a green to orange appearance, depending on the developmental stage of the spores (Tab 1). Clearly visible in our spectral data, both *Chloromonas* sp. contained less astaxanthins, making them clearly distinguishable from *Chlamydomonas nivalis* in hyperspectral mapping image. Hyperspectral technology may thus be also applied to discriminate mixed samples of algae, which is most often the case [36]. These authors used diatoms and green algae of known ratio to study spectral shifts derived from different contributing pigments, without however showing the mapping of the measured spectra. One of the first reports to use hyperspectral imaging for discriminating among different photosynthetic organisms was applied in corals, but not by a microscopic approach [37].

4.2 Distribution of pigments in algae

In our study we demonstrate, that a discrimination between signals derived from different pigments (e.g. astaxanthins, chlorophyll) can be achieved using hyperspectral mapping on single-celled algae. Different chloroplast shapes lead to a distinct appearance of the various streptophytic green algae used in our study. The star shaped chloroplasts from *Zygnema* sp. [16], were clearly distinct from the parietal chloroplasts found in *Klebsormidium crenulatum* [14]. For technical reasons we could not capture absorbance below 400 nm (the filters within the Nikon Eclipse 80i microscope did not allow transmittance of light with wavelengths < 400 nm). Therefore, we could not determine any strictly UV absorbing compounds, like phenolic compounds (see Tab. 1), which are present e.g. in *Zygnema* sp. or *Zygogonium erictorum* [4, 6]. The absorption maximum of the phenolic compound of the latter species was determined at 270-280 nm [17], and is thus below the spectral range of the current microscopic application with PARISS® hyperspectral imaging. *Zygogonium ericetorum* has a distinct cell architecture, with large vacuoles containing a ferric $(gallate)_2$ complex that causes the purple color [38]. Recently an iron exclusion mechanism via the phenolic has been proposed in *Z. ericetorum* by [6].

The pigment composition however, might be determined and used as an exclusion criterion for a certain stage of culture development, as previously demonstrated for *Haematococcus pluvialis* [39–40]. During the life cycle, these algae change their pigment composition; while in zoospores astaxanthin was localized in the eyespot, it became widely distributed in the cells, but localized differently than chlorophyll. The hyperspectral technique applied for these investigations [40] was different from the PARISS® approach used in our study, where the spectral information was collected simultaneously across the entire spectrum. There, the light was transmitted through a liquid crystal tuneable filter (LCTF), photons passing through this LCTF at each wavelength were captured with an electron multiplying charge coupled device (EMCCD) camera to obtain the hyperspectral images [40]. By the use of a multivariate curve resolution to the hyperspectral image data, it was demonstrated that the predicted values correlate with the actual measurements of extracted pigments [34]. Label-free measurements of algal triacylgylceride production has been recently achieved via fluorescence hyperspectral imaging in a variety of microalgae, e.g. *Nannochloropsis* sp.

Dunaliella salina, *Neochloris oleoabundans*, *Chlamydomonas reinhardtii* [41]. *In vivo* hyperspectral confocal fluorescence imaging was previously used to determine pigment distribution in cyanobacteria [42].

4.3 Osmotic changes and desiccation

Water loss is a potential threat in snow algae and aeroterrestrial green algae [18], and was therefore applied in the present study to analyze if the spectral properties change during this treatment. Snow algae were remarkably resistant against osmotic stress, and not even 1,600 mM sorbitol caused a visible plasmolysis. Consequently, the spectral properties did not change even during these high concentration of osmoticum. In contrast, physical drying at ambient air caused an accumulation of snow algae leading to an increased absorbance, a scenario that might occur in nature when the snow fields are melting during summer and the algae end up on the soil surface. Plasmolysis, induced by osmotic treatment had severe effects on different *Zygnema* sp. and *Klebsormidium* sp. [21, 23]. The relative volume changes as a consequence of drying can be as drastic as 50% of the initial volume determined in *Zygnema* sp. and *Klebsormidium crenulatum* [43]. The absorbance increased in plasmolysed and desiccated samples, particularly in the lower waveband of 400-500 nm due to the higher density of the pigments. These changes might be ecologically relevant, as aeroterrestrial algae are naturally exposed to occasional water limitation, leading to desiccation, and also high irradiance particularly at high altitudes where these algae naturally occur. However, this effect was not observed in *Zygogonium ericetorum* [17]. The osmotic treatments had another advantage for the analysis; the absorbance of the cell walls, which were clearly separated from the protoplast could be studied. It became particularly clear, that neither the cell walls nor the spaces between the retracted protoplast did have distinct spectral properties in the range observed (400-900 nm).

Our findings demonstrate the capacity of the hyperspectral (PARISS®) technology that has previously been successfully applied to different systems like bio-inspired structural color analysis [44], biophotonic properties of shrimps [45] or properties of capillary foams [46]. From our results we can conclude the technique will be useful in different applications concerning algal or phytoplankton research; the chloroplast shapes with different morphologies might be used to select a given composition of a sample and automated approaches could help to count cells of a given species. Hyperspectral imaging could also be used in the future to address the dynamic change between spectra and organelles upon exposure to specific experimental stress conditions. Currently MicroSpectroPhotometry (MSP) is the most widely used method to perform spatial analysis of spectra, e.g. in cotton fibers [47]. Using MSP, spectra are recorded from area of sample using small optical fibers that record spectra from the area only, without spatial discrimination within the area. MSP is applicable mostly for large size samples, and is not applicable because of the lack of spatial resolution at the level of small sample size like the case for single cell algae. Hyperspectral imaging fills this gap.

As demonstrated with the mixed snow algal sample, it is easy to distinguish between different species with distinct spectral properties. In future studies, an expansion of the

investigated waveband below 400 nm could give valuable insights in the occurrence and distribution of ecophysiologically relevant UV protecting substances.

Acknowledgements

Our sincere thanks go to Dr. Daniel Remias, FH Wels, Austria for collecting the field sample of WP 79 and several helpful discussions during the preparation of the manuscript. The study was supported by a travelling grant from the 'Foreign Relation Office' of the University of Innsbruck and FWF grants P 24242-B16 and I 1951-B16 to AH. The hyperspectral imager was funded by the Air Force Office of Scientific Research (AFOSR) grant # FA9550-10-1-0555 (MURI BIOPAINTS) to DDD.

References

[1]. Remias D, Lütz-Meindl U, Lütz C. Photosynthesis, pigments and ultrastructure of the alpine snow alga *Chlamydomonas nivalis*. Eur J Phycol. 2005; 40:259–268.

[2]. Holzinger A, Lütz C. Algae and UV irradiation: Effects on ultrastructure and related metabolic functions. Micron. 2006; 37:190–207. [PubMed: 16376552]

[3]. Karsten U, Holzinger A. Green algae in alpine biological soil crust communities – Acclimation strategies against ultraviolet radiation and dehydration. Biodivers Conserv. 2014; 23:1845–1858. [PubMed: 24954980]

[4]. Aigner S, Remias D, Karsten U, Holzinger A. Unusual phenolic compounds contribute to the ecophysiological performance in the purple-colored green alga *Zygogonium ericetorum* (Zygnematophyceae, Streptophyta) from a high-alpine habitat. J Phycol. 2013; 49:648–660. [PubMed: 25810559]

[5]. Herburger K, Remias D, Holzinger A. The green alga *Zygogonium ericetorum* (Zygnematophyceae, Charophyta) shows high iron and aluminium tolerance: Protection mechanisms and photosynthetic performance. FEMS Microbiol Ecol. 2016; doi: 10.1093/femsec/fiw103

[6]. Pichrtová M, Remias D, Lewis LA, Holzinger A. Changes in phenolic compounds and cellular ultrastructure of arctic and Antarctic strains of *Zygnema* (Zygnematales, Streptophyta) after exposure to experimentally enhanced UV to PAR ratio. Microb Ecol. 2013; 65:68–83. [PubMed: 22903087]

[7]. Kitzing C, Pröschold T, Karsten U. UV-induced effects on growth, photosynthetic performance and sunscreen contents in different populations of the green alga *Klebsormidium fluitans* (Streptophyta) from alpine soil crusts. Microb Ecol. 2014; 67:327–340. [PubMed: 24233286]

[8]. Holzinger A, Pichrtová M. Abiotic stress tolerance in charophyte green algae: New challenges for omics techniques. Front Plant Sci. 2016; 7:678.doi: 10.3389/fpls.2016.00678 [PubMed: 27242877]

[9]. Remias D, Lütz C. Characterization of esterified secondary carotenoids and the isomers in green algae: a HPLC approach. Algol Stud. 2007; 124:85–94.

[10]. Remias D, Pichrtová M, Pangratz M, Lütz C, Holzinger A. Ecophysiology, secondary pigments and ultrastructure of *Chlainomonas* sp. (Chlorophyta) from the European Alps compared to *Chlamydomonas nivalis* forming red snow. FEMS Micorbiol Ecol. 2016; doi: 10.1093/femsec/fiw030

[11]. Remias, D. Cell structure and physiology of alpine snow and ice algae. Plants in Alpine Regions: Cell Physiology of Adaptation and Survival Strategies. Lütz, C., editor. Springer Verlag; Wien, New York: 2012. p. 175-186.

[12]. Lutz S, Anesio AM, Field K, Benning LG. Integrated 'Omics', targeted metabolite and single-cell analyses of arctic snow algae functionality and adaptiability. Front Microbiol. 2015; 6:1323.doi: 10.3389/fmicb.2015.01323 [PubMed: 26635781]

[13]. Remias D, Schwaiger S, Aigner S, Leya T, Stuppner H, Lütz C. Characterization of an UV- and VIS-absorbing, purpurogallin-derived secondary pigment new to algae and highly abundant in *Mesotaenium berggrenii* (Zygnematophyceae, Chlorophyta), an extremophyte living on glaciers. FEMS Microbiol Ecol. 2012; 79:638–648. [PubMed: 22092588]

Europe PMC Funders Author Manuscripts

Europe PMC Funders Author Manuscripts

[14]. Remias D, Lütz C, Karsten U, Leya T. Physiological and morphological processes in the Alpine snow alga *Chloromonas nivalis* (Chlorophyceae) during cyst formation. Protoplasma. 2010; 243:73–86. [PubMed: 20229328]

[15]. Karsten U, Lütz C, Holzinger A. Ecophysiological performance of the aeroterrestrial green alga *Klebsormidium crenulatum* (Charophyceae, Streptophyta) isolated from an alpine soil crust with an emphasis on desiccation stress. J Phycol. 2010; 46:1187–1197.

[16]. Herburger K, Lewis LA, Holzinger A. Photosynthetic efficiency, desiccation tolerance and ultrastructure in two phylogenetically distinct strains of alpine *Zygnema* sp. (Zygnematophyceae, Streptophyta): Role of pre-akinete formation. Protoplasma. 2015; 252:571–589. [PubMed: 25269628]

[17]. Holzinger A, Tschaikner A, Remias D. Cytoarchitecture of the desiccation-tolerant green alga *Zygogonium ericetorum*. Protoplasma. 2010; 243:15–24. [PubMed: 19449090]

[18]. Stancheva R, Hall JD, Herburger K, Lewis LA, McCourt RM, Sheath RG, Holzinger A. Phylogenetic position of *Zygogonium ericetorum* (Zygnematophyceae, Charophyta) from a high alpine habitat and ultrastructural characterization of unusual aplanospores. J Phycol. 2014; 50:790–803. [PubMed: 25810560]

[19]. Gray DW, Lewis LA, Cardon ZG. Photosynthetic recovery following desiccation of desert green algae (Chlorophyta) and their aquatic relatives. Plant Cell Environ. 2007; 30:1240–1255. DOI: 10.1111/j.1365-3040.2007.01704.x [PubMed: 17727415]

[20]. Holzinger A, Lütz C, Karsten U. Desiccation stress causes structural and ultrastructural alterations in the green alga *Klebsormidium crenulatum* (Klebsormidiophyceae, Streptophyta) isolated from an alpine soil curst. J Phycol. 2011; 47:591–602. [PubMed: 27021989]

[21]. Kaplan F, Lewis LA, Wastian J, Holzinger A. Plasmolysis effects and osmotic potential of two phylogenetically distinct alpine strains of *Klebsormidium* (Streptophyta). Protoplasma. 2012; 249:789–804. [PubMed: 21979310]

[22]. Karsten U, Holzinger A. Light, temperature and desiccation effects on photosynthetic activity and drought-induced ultrastructural changes in the green alga *Klebsormidium dissectum* (Streptophyta) from a high alpine soil crust. Microb Ecol. 2012; 63:51–63. [PubMed: 21811791]

[23]. Kaplan F, Lewis LA, Herburger K, Holzinger A. Osmotic stress in the arctic and antarctic green alga *Zygnema* sp. (Zygnemtales, Streptophyta): Effects on photosynthesis and ultrastructure. Micron. 2013; 44:317–330. [PubMed: 22959821]

[24]. Holzinger A, Karsten U. Desiccation stress and tolerance in green algae: Consequences for ultrastructure, physiological, and molecular mechanisms. Front Plant Sci. 2013; 4doi: 10.3389/fpls.2013.00327

[25]. Clark CD, Mumby PJ, Chisholm JRM, Jaubert J, Andrefouet S. Spectral discrimination of coral mortality states following a severe bleaching event. Int J Remote Sens. 2000; 21:2321–2327.

[26]. Blackburn GA. Hyperspectral remote sensing of plant pigments. J Exp Bot. 2007; 58:855–867. DOI: 10.1093/Jxb/Erl123 [PubMed: 16990372]

[27]. Torres-Perez JL, Guild LS, Armstrong RA. Hyperspectral distinction of two caribbean shallow-water corals based on their pigments and corresponding reflectance. Remote Sens. 2012; 4:3813–3832.

[28]. van der Meer FD, et al. Multi- and hyperspectral geologic remote sensing: A review. Int J Appl Earth Obs. 2012; 14:112–128. DOI: 10.1016/J.Jag.2011.08.002

[29]. Yao-hua L, Ke G, Zhong-ping T, Mao-zhi W. The application research of Hyperspectral remote sensing technology in tailing mine environment pollution supervise management. IEEE. 2012 Doi: 978-1-4673-0875-5/12.

[30]. Kobryn HT, Wouters K, Beckley LE, Heege T. Ningaloo reef: Shallow marine habitats mapped using a hyperspectral sensor. PLoS One. 2013; 8doi: 10.1371/journal.pone.0070105

[31]. Olmanson LG, Brezonik PL, Bauer ME. Airborne hyperspectral remote sensing to assess spatial distribution of water quality characteristics in large rivers: The Mississippi River and its tributaries in Minnesota. Remote Sens Environ. 2013; 130:254–265. DOI: 10.1016/J.Rse.2012.11.023

[32]. Fassnacht FE, Latifi H, Ghosh A, Joshi PK, Koch B. Assessing the potential of hyperspectral imagery to map bark beetle-induced tree mortality. Remote Sens Environ. 2014; 140:533–548. DOI: 10.1016/j.rse.2013.09.014

[33]. Tochon G, Feret J-B, Valero S, Asner GP. On the use of binary partition trees for the tree crown segmentation of tropical rainforest hyperspectral images. Remote Sens Environ. 2015; 159:318–331. DOI: 10.1016/j.rse.2014.12.020

[34]. Millan VEG, Sanchez-Azofeifa GA, Malvarez GC. Mapping Tropical Dry Forest Succession With CHRIS/PROBA Hyperspectral Images Using Nonparametric Decision Trees. IEEE J-Stars. 2015; 8:3081–3094. DOI: 10.1109/Jstars.2014.2365180

[35]. Fagan M, DeFries RS, Sesnie SE, Arroyo-Mora JP, Soto C, Singh A, Twonsend PA, Chazdon RL. Mapping Species Composition of Forests and Tree Plantations in Northeastern Costa Rica with an Integration of Hyperspectral and Multitemporal Landsat Imagery. Remote Sens. 2015; 7:5660–5696. DOI: 10.3390/rs70505660

[36]. Mehrubeoglu M, Teng MY, Zimba PV. Resolving mixed algal species in hyperspectral images. Sensors. 2014; 14:1–21.

[37]. Barott K, Smitz J, Dinsdale E, Hatay M, Sandin S, Rohwer F. Hyperspectral and physiological analyses of coral-algal interactions. PLoS ONE. 2009; 4(11):e8043. [PubMed: 19956632]

[38]. Newsome AG, Murphy BT, van Breemen RB. Isolation and characterization of natural blue pigments from underexplored sources. Phys Meth Food Analysis. 2013; 1138:105–125.

[39]. Collins AM, Jones HDT, Han D, Hu Q, Beechem TE, Timlin JA. Carotenoid distribution in living cells of *Haematococcus pluvialis* (Chlorophyceae). PLoS ONE. 2011; 6(9):e24302. [PubMed: 21915307]

[40]. Nogami S, Ohnuki S, Ohya Y. Hyperspectral imaging techniques for the characterization of *Haematococcus pluvialis* (Chlorophyceae). J Phycol. 2014; 50:939–947. [PubMed: 26988647]

[41]. Davis RW, Jones HDT, Collins AM, Ricken JB, Sinclair MB, Timlin JA, Singh S. Label-free measurement of algal triacylglyceride production using fluorescence hyperspectral imaging. Algal Res. 2014; 5:181–189.

[42]. Vermaas WFJ, Timlin JA, Jones HDT, Sinclair MB, Nieman LT, Hamad SW, Melgaard DK, Haaland DM. *In vivo* hyperspectral confocal fluorescence imaging to determine pigment localization and distribution in cyanobacterial cells. Proc Natl Acad Sci USA. 2007; 105:4050–4055.

[43]. Lajos K, Mayr S, Buchner O, Blaas K, Holzinger A. A new microscopic method to analyse desiccation induced volume changes in aeroterrestrial green algae. J Microscopy. 2016; doi: 10.1111/jmi.12409

[44]. Xiao M, Li Y, Allen MC, Deheyn DD, Yue X, Zhao J, Gianneschi NC, Shawkey MD, Dhinojwala A. Bio-inspired structural colors produced via self-assembly of synthetic melanin nanoparticles. ACS Nano. 2015; 9:5454–5460. [PubMed: 25938924]

[45]. Taylor JRA, Gilleard JM, Allen MC, Deheyn DD. Effects of CO_2 induced pH reduction on the exoskeleton and biophotonic properties of the shrimp *Lysmata californica* . Scientific Reports. 2015; 5:10608.doi: 10.1038/srep10608 [PubMed: 26030212]

[46]. Zhang Y, Allen MC, Zhao R, Deheyn DD, Behrens SH, Meredith JC. Capillary foams: Stabilization and functionalization of porous liquids and solids. Langmuir. 2015; doi: 10.1021/la504784h

[47]. Was-Gubala J, Starczak R. UV-Vis microspectrophotometry as a method of differentiation between cotton fibre evidence coloured with reactive dyes. Spectrochim Acta A Mol Biomol Spectrosc. 2015; 142:118–125. [PubMed: 25699701]

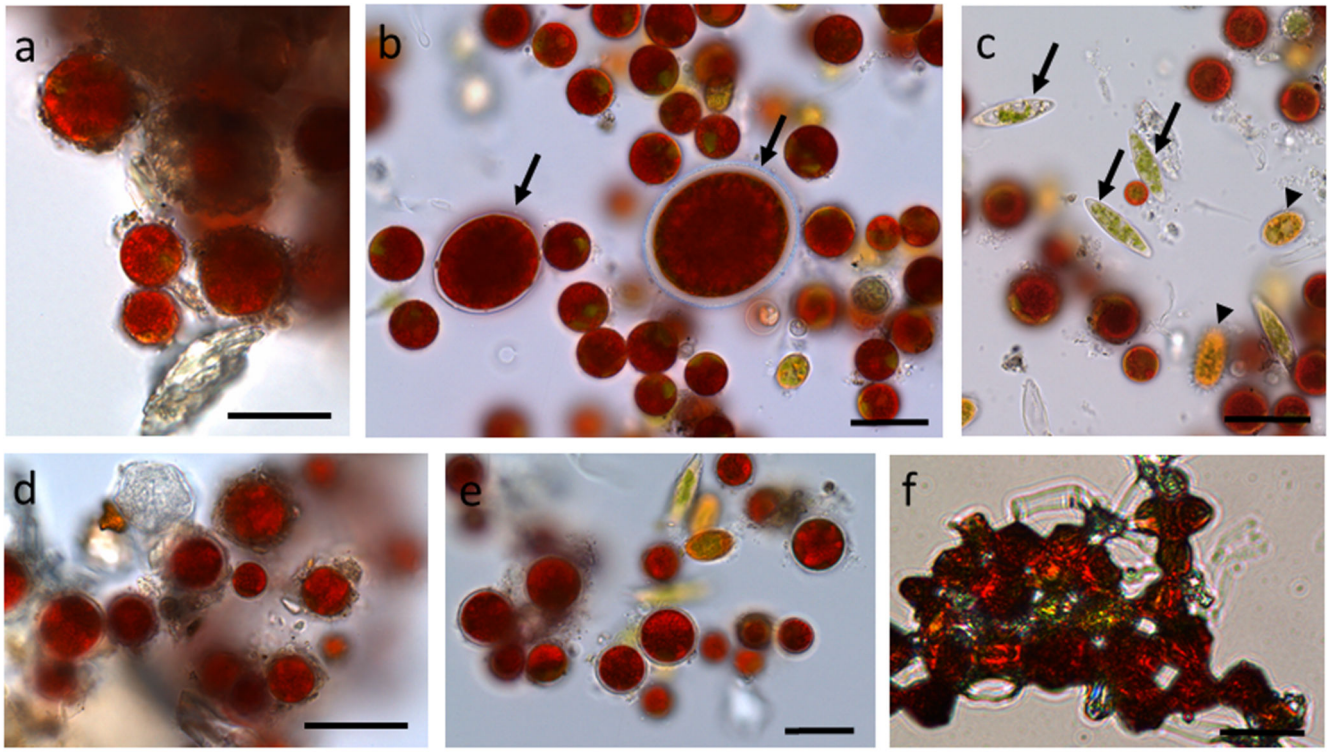

Fig. 1.

Light microscopy of snow algal cells from different field samples (S1, a, d) and (WP79 b-c, e-f). (a) *Chlamydomonas nivalis* covered with debris, (b) *Chlamydomonas nivalis*, *Chlainonmonas* sp. cells are marked with an arrow, (c) *Chloromonas rosae* var. *psychrophila* (arrows), *Chloromonas brevispina* (arrowheads), (d) sample S1 plasmolysed in 1,600 mM sorbitol, (e) sample WP79 plasmolysed in 1,600 mM sorbitol, (f) sample WP79 desiccated. Bars 20 μm

Europe PMC Funders Author Manuscripts

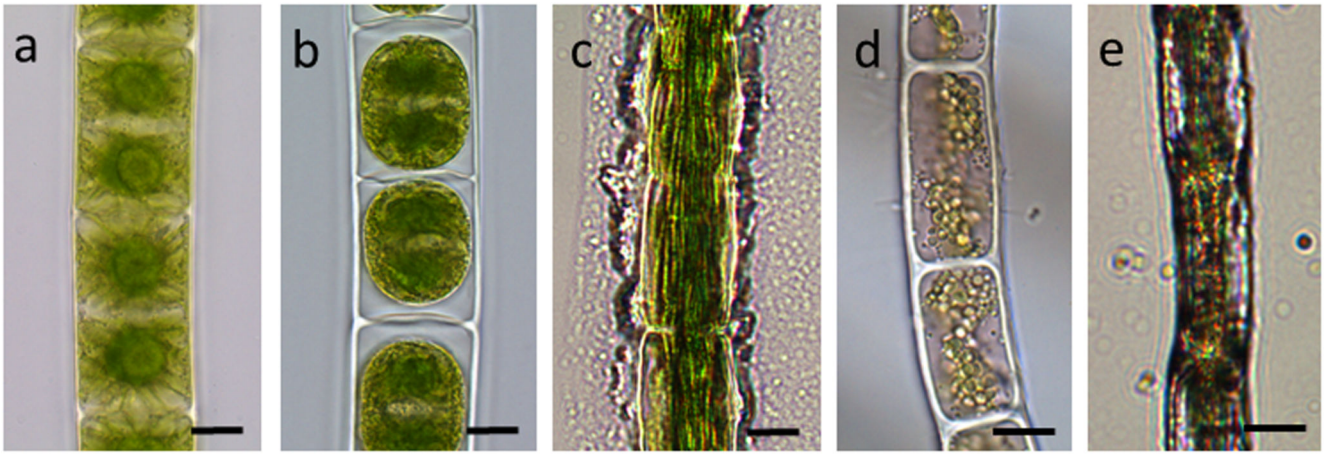

Fig. 2.

Cultivated cells of (a) *Zygnema* sp., (b) *Zygnema* sp. plasmolysed with 800 mM sorbitol, (c) *Zygnema* sp. desiccated, severe damage of the cells, (d) *Zyogogonium ericetorum* field sample, (e) *Zyogogonium ericetorum* air dried. Bars 20 μm

Europe PMC Funders Author Manuscripts

Europe PMC Funders Author Manuscripts

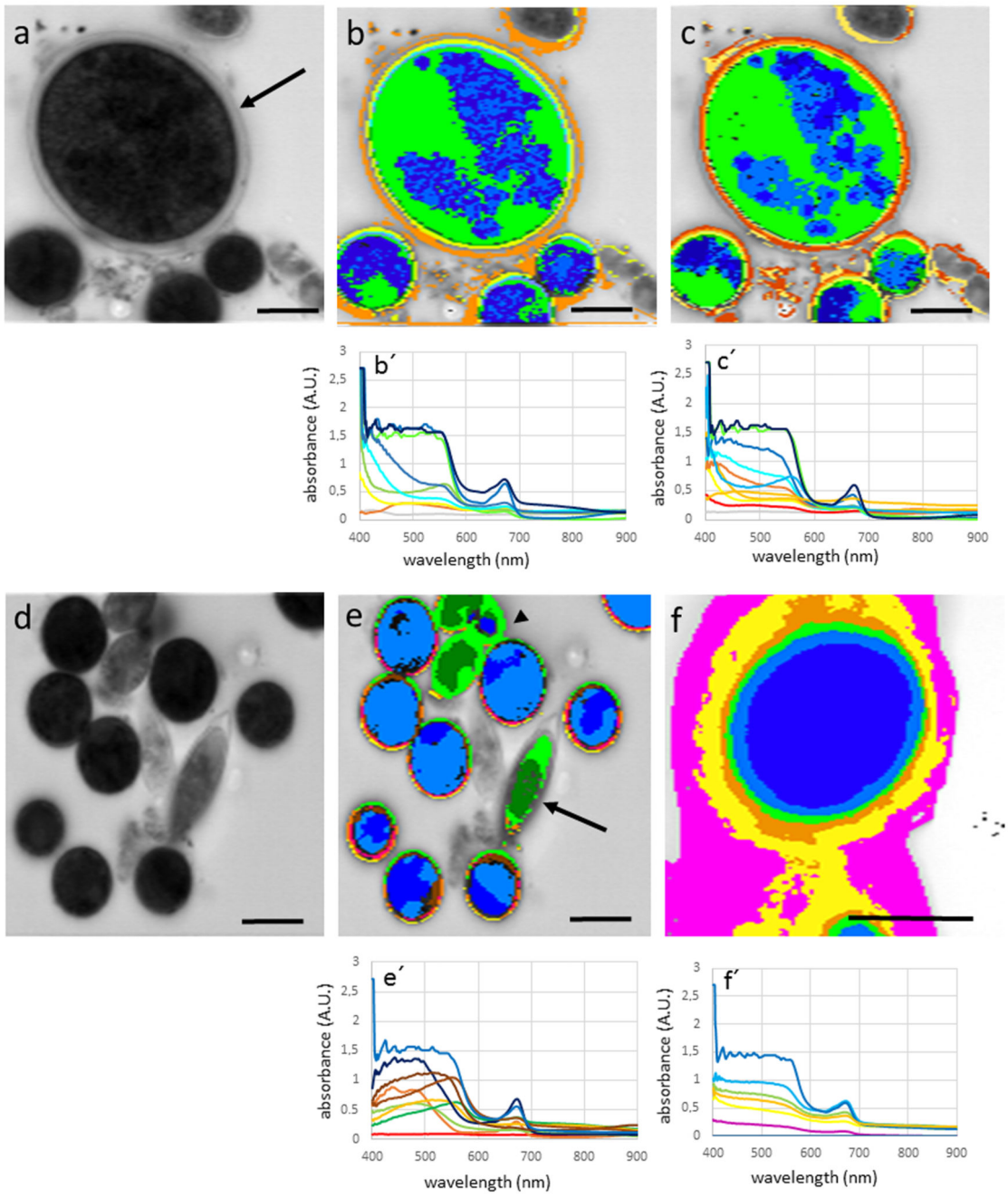

Fig. 3.

Hyperspectral images and corresponding spectra (below) of snow algae. (a) *Chlainomonas* sp. (arrow) and *Chlamydomonas nivalis* cells, bright field image, (b) hyperspectral image of the same cell with Min CC: 0.985, (c) hyperspectral image calculated with Min CC: 0.99, (d) bright field image of field sample (WP97) containing *Chlamydomonas nivalis* and *Chloromonas brevispina* (arrowhead) and *Chloromonas rosae* var. *psychrophila* (arrowhead), note the different spectral properties of the latter two, (f) *Chlamydomonas nivalis* from sampling site (S1). Bars 10 μm

Europe PMC Funders Author Manuscripts

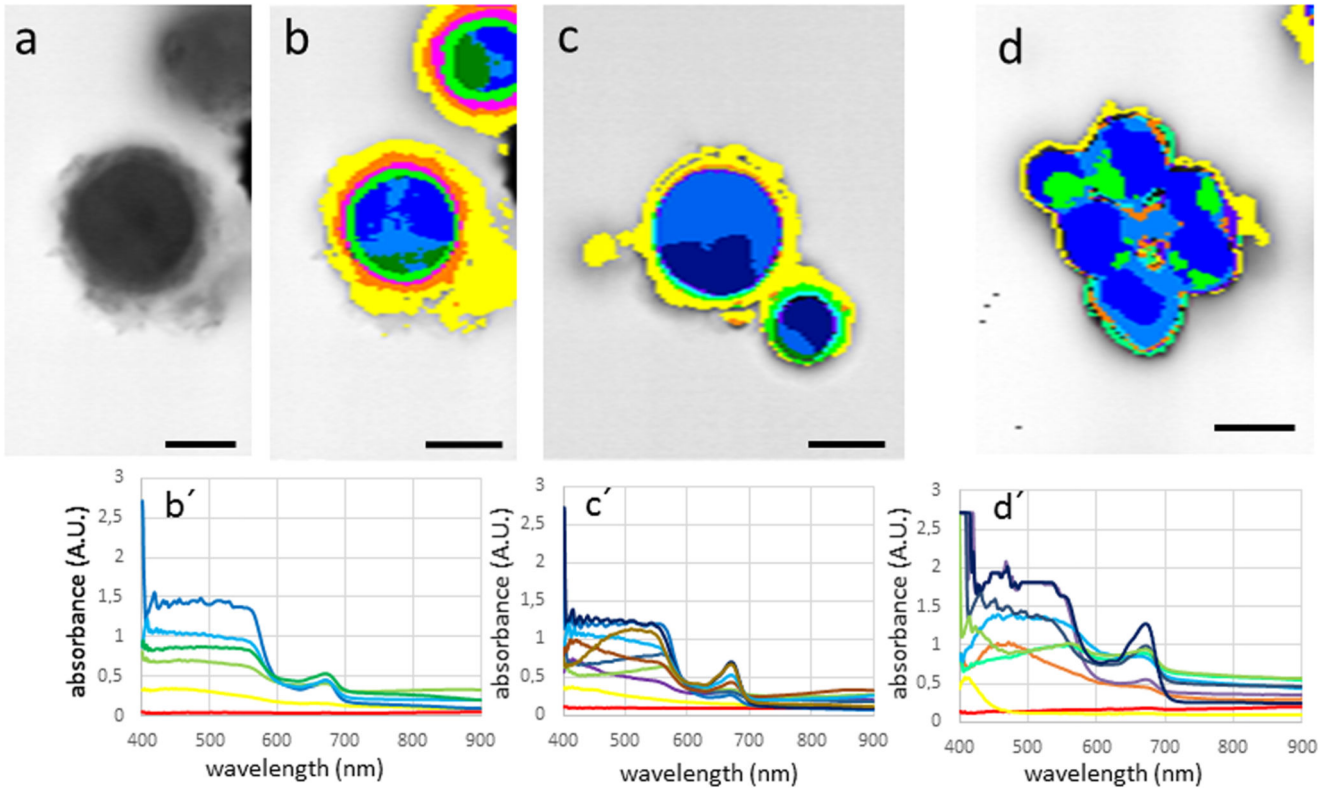

Fig. 4.

Hyperspectral images and corresponding spectra (below) of *Chlamydomonas nivalis* (a) bright field image of cells plasmolysed with 800 mM sorbitol, (b) hyperspectral image of the same cells, (c) plasmolysed with 1600 mM sorbitol, (d) desiccated in ambient air. Bars 10 μm

Europe PMC Funders Author Manuscripts

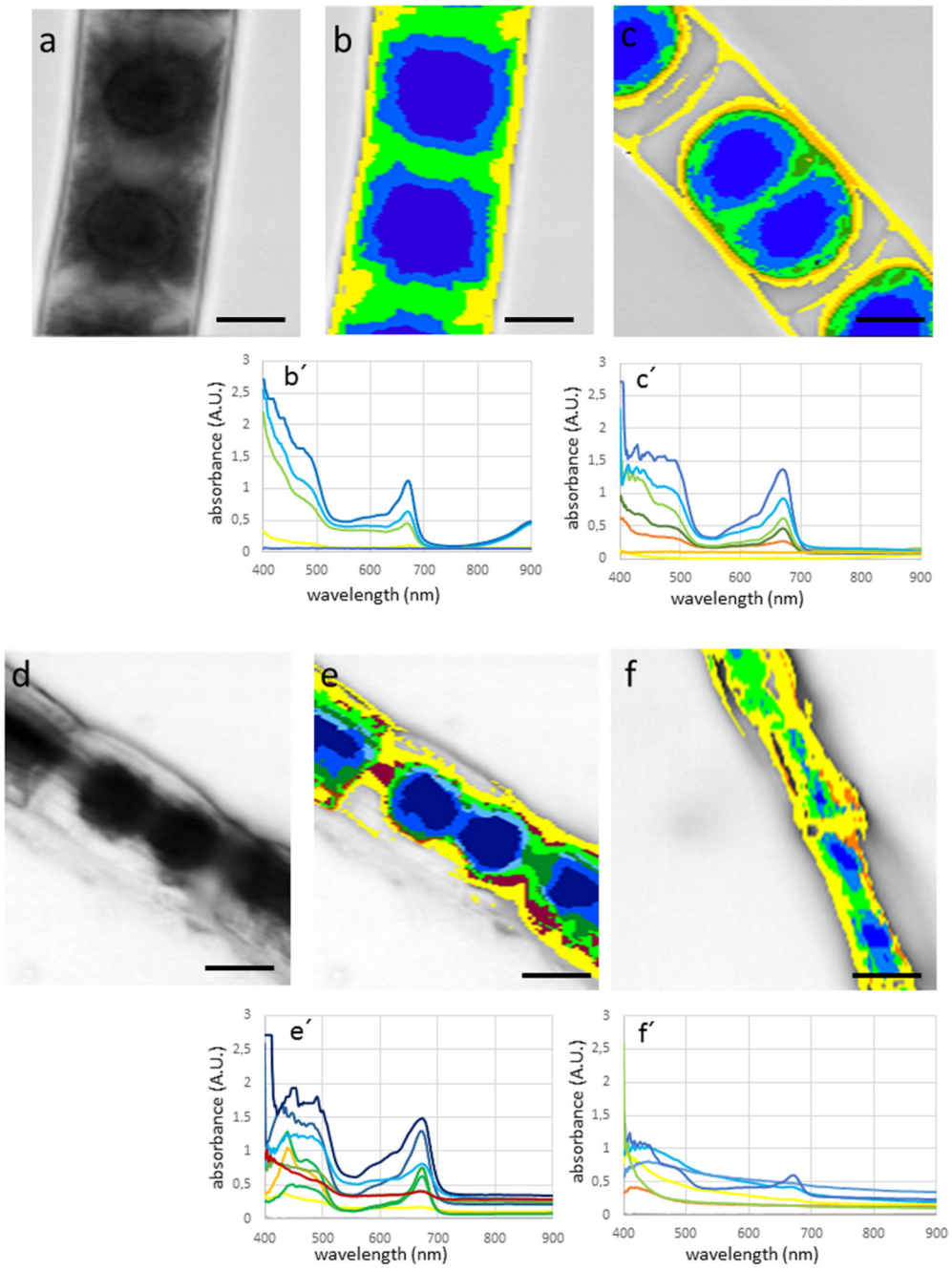

Fig. 5.

Hypersectral images and corresponding spectra (below) of *Zygnema* sp. (A-E) and *Zygogonium ericetorum* (F) cells. (a) bright field image, (b) hyperspectral image of the same cell, (c) cells plasmoylsed in 800 mM sorbitol, retraction of the protoplast, (d) bright field image of air dried cells, (e) corresponding hyperspectral image, (f) desiccated cell of *Zygogonium ericetorum*, note the irregular shrinkage of the cells. Bars 10 µm

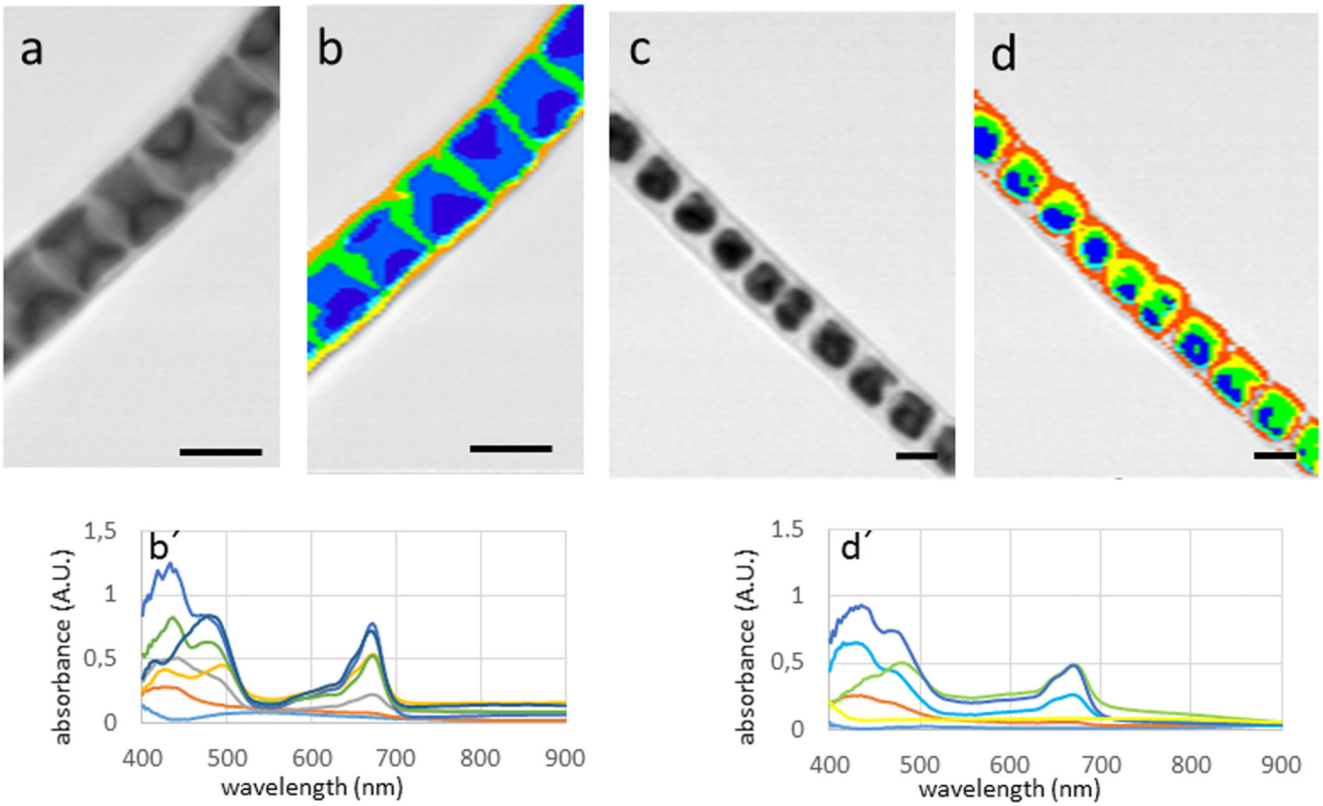

Fig. 6.

Hyperspectral images and corresponding spectra (below) of *Klebsormidium crenulatum*. (a) bright-field image, (b) corresponding hyperspectral image, (c) cells plasmolysed with 800 mM sorbitol, note the retraction of the cytoplasm, (d) corresponding hyperspectral image. Bars 10 μm.

Europe PMC Funders Author Manuscripts

Europe PMC Funders Author Manuscripts

Tab. 1

Summary of investigated algae, characterizing their developmental state, origin and pigment composition

Genus	*Developmental stage*	*Field sample*	*Culture*	*Secondary carotenoids*	*Phenolics*
Chlamydomonas nivalis	mature spores	WP 79, S1		++	
Chlainomonas sp.	mature spores	WP 79		++	
Chloromonas rosae	mature spores	WP 79		+	
Chloromonas brevisp.	mature spores	WP 79		+	
Klebsormidium crenul.	vegetative cells		SAG 2515		
Zygnema sp.	vegetative cells		SAG 2419		+
Zygogonium ericet.	vegetative cells	S1			+